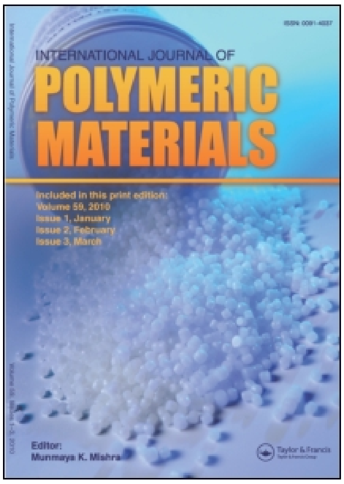

International Journal of Polymeric Materials
Publication details, including instructions for authors and subscription information:
http://www.informaworld.com/smpp/title~content=t713647664

General formula for optical characterization of multi-elliptical core optical fibers with microscopic interferometry

A. M. Sadik[a]
[a] Optical Research Group, Physics Department, Faculty of Science, University of Mansoura, Mansoura, Egypt

Online publication date: 27 October 2010

To cite this Article Sadik, A. M.(2003) 'General formula for optical characterization of multi-elliptical core optical fibers with microscopic interferometry', International Journal of Polymeric Materials, 52: 9, 761 — 772
To link to this Article: DOI: 10.1080/713743714
URL: http://dx.doi.org/10.1080/713743714

International Journal of Polymeric Materials, 52:761–772, 2003

ISSN: 0091-4037 print/1543-5253 online
DOI: 10.1080/00914030390225084

GENERAL FORMULA FOR OPTICAL CHARACTERIZATION OF MULTI-ELLIPTICAL CORE OPTICAL FIBERS WITH MICROSCOPIC INTERFEROMETRY

A. M. Sadik
Optical Research Group, Physics Department, Faculty of Science, University of Mansoura, Mansoura, Egypt

In the present paper, the interference pattern of multi-elliptical core optical fiber in a transverse interferometer has been described by a general interference formula. This formula with Mach-Zehnder interferometry is used to characterize multi-elliptical core optical fiber via its refractive index measurement. Example of application to identical nine-elliptical core optical fiber of thickness 380 microns is given.

Keywords: optical fiber, refractive index, refractive index profile, Mach-Zehnder interferometer, multi-elliptical core

INTRODUCTION

The organic or inorganic optical fiber is a dielectric waveguide structure that transports energy at a certain wavelength in the infrared or visible portion of the electromagnetic spectrum. In general, optical waveguides have a skin-core structure: the core must has greater value of refractive index than the cladding in order to satisfy the guidance conditions. The cladding refractive index is always constant, and the core may have constant or graded index across the fiber radius.

Recent interest in the production of long low-loss fibers for imaging or telecommunication purposes has prompted the development of

Received 15 April 2001; in final form 22 April 2001.

The author expresses his appreciation to Prof. A. A. Hamza, the president of Mansoura University for his useful discussions. Also, the author is grateful to Mr. Marek Wychowaniec, Applied Optics Institute (IOS)-Warsaw, for friendship and cooperation.

Address correspondence to A. M. Sadik, Optical Research Group, Physics Department, Faculty of Science, University of Mansoura, 35516, Mansoura, Egypt. E-mail: adelsa_12@yahoo.com

sensitive methods to characterize the parameter of such fibers. The measured optical parameters of these fibers are affected strongly by the method of calculation. Different techniques have been proposed and described to determine the refractive index profiles and index difference of optical fibers and microinterferometry is considered one of most accurate among them. Two interferometric techniques are distinguished: slab or axial interferometry [1, 2] and transverse interferometry [3−14]. Quite recently, the multiple-beam interference technique [15−16] has been applied in transverse optical fiber profiling.

In transverse interferometric refractive index profiling methods, the investigated axially symmetric phase object is illuminated transversly to its axis. Up to now the required data were commonly extracted from the interference fringe deviation observed in the Mach-Zehnder or other fringe-field interferometer [6−15]. Mach-Zehnder interferometer is often used for index profile measurement in which the object under study is placed in one of its optical paths. In the present work, computer-aided Mach-Zehnder interferometer and general interference formula for determining the optical properties of nine-elliptical core optical fibers are used. Also, they can detect possible optical, and geometrical microdefects of these fibers *via* their fringe shift distribution along their lengths.

OPTICAL SYSTEM

Mach-Zehnder interferometer is shown schematically in Figure 1. Laser source **S** illuminates narrow slit that is positioned at the focal plane of corrected lens $\mathbf{L_1}$. A beam of plane parallel light is divided at the semi-reflecting surface of plane parallel glass plate $\mathbf{D_1}$ into two beams. These beams are reflected at plane mirrors $\mathbf{M_1}$ and $\mathbf{M_2}$ and they are recombined at the semi-reflecting surface of a second plane parallel glass plate $\mathbf{D_2}$. Finally they emerge to a corrected lens $\mathbf{L_2}$ and interfere with each other producing an interference pattern that can be captured by CCD camera. An investigated optical fiber is placed in a quartz cell $\mathbf{C_2}$ and introduced in one of the optical paths of the Mach-Zehnder interferometer. The fiber under study is immersed in a liquid whose refractive index $\mathbf{n_L}$ is nearly close to that of the fiber cladding. A compensating quartz cell $\mathbf{C_1}$ of the same liquid is inserted in the second optical path of the Mach-Zehnder interferometer. To provide smooth rotation of the multi-elliptical core optical fiber, a rotating table that has a special mechanism is used. It is possible to measure the fringe shift in a selected core. Particular fiber regions fulfilling the measurement conditions of this method can be obtained by turning the fiber round its main axis through an angle arising from its geometry

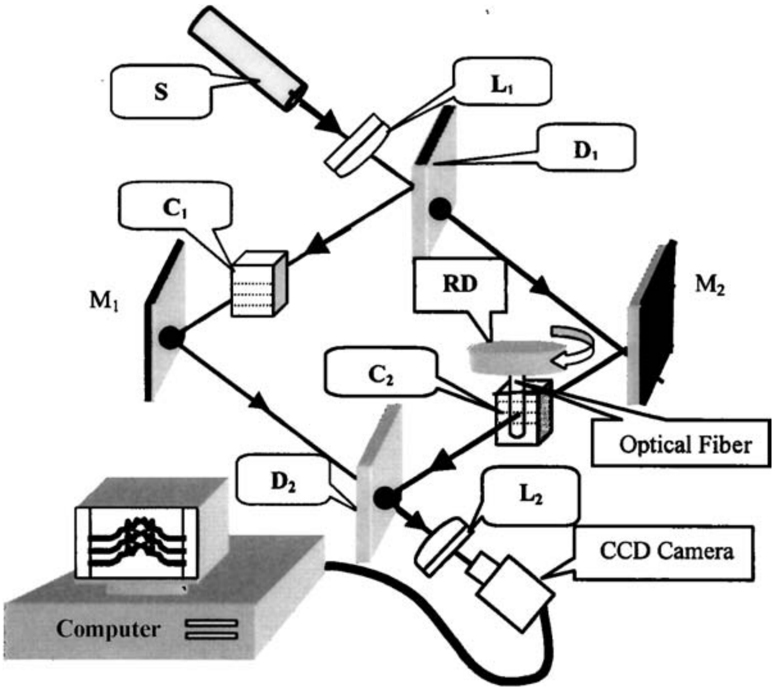

FIGURE 1 Schematic diagram of computer-aided Mach-Zehender interferometer; laser beam source **S**, two lenses $\mathbf{L_1}$ and $\mathbf{L_2}$, two reflected mirrors $\mathbf{M_1}$ and $\mathbf{M_2}$, two beam splitters $\mathbf{D_1}$ and $\mathbf{D_2}$, rotating disk **RD**, two liquid quartz cells $\mathbf{C_1}$ and $\mathbf{C_2}$, **CCD** camera, and **PC** compatible computer.

(Fig. 2). The interference pattern of the output field is collected by a CCD camera for further automatic processing and analysis by the computer system.

THEORY

In general, the intensity distribution that is observed in the exit plane of any interferometer can be described as follows:

$$\mathbf{I} = \mathbf{I_T} + \mathbf{I_c}\,\mathbf{cos}[\Delta(\mathbf{x},\mathbf{y}) - \Phi] \quad (1)$$

Where I_T is the background intensity, I_c is the interference pattern amplitude governing the image contrast, $\Delta(x, y)$ is the phase change introduced by investigated object, and Φ is the bias, that is the phase difference between the interfringe wavefronts. When Φ is a constant, the observed field is homogenous (in the absence of $\Delta(x, y)$; empty

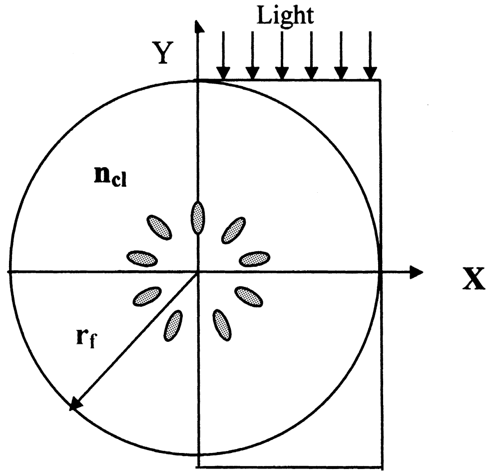

FIGURE 2 Displays the schematic diagram of the cross section of the identical nine elliptical core optical fiber.

field). When Φ is function of space coordinates, fringe appears, that will be perturbed by the presence of the object introduced phase retardation Δ(x, y). From the form of Eq. (1) it follows that the intensity I in any interferogram is a periodic function of the bias Φ with 2π period. The phase shift of a probing beam is detected as fringe shift and the refractive index profile is calculated from fringe shift distribution. The optical path length "Γ(x, y)" covered by the illumination wave while traversing the object under study can be given by

$$\Gamma(x, y) = \frac{\lambda}{2\pi}\Delta(x, y) \tag{2}$$

General interference formula for measuring the refractive index and index profile of cylindrical optical fiber having an identical multi-elliptical cores with the Mach-Zehnder interferometer will be derived. We assume a cross-section of a cylindrical optical fiber of radius r_f having nine identical elliptical cores of radii ρ_1 (major axis) and ρ_2 (minor axis) and constant refractive index n_c and cladding of refractive index n_{cl} (see Fig. 2). At the beginning, we will deal with the simplest cases as follows:

(i) Let us assume that the optical fiber is of radius r_f having an elliptical core of constant refractive index $\mathbf{n_c}$ and radii "ρ_1" and "ρ_2" and a cladding of constant refractive index $\mathbf{n_{cl}}$ as shown in

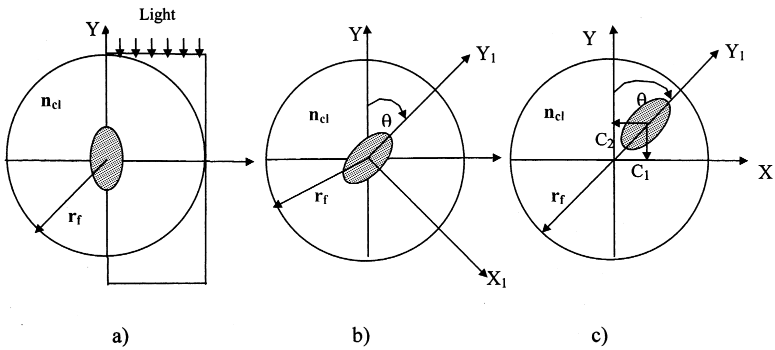

FIGURE 3 Displays the schematic diagram of the cross sections of different types of the elliptical core optical fibers.

Figure 3a. This fiber is immersed in cell and introduced in one arm of the Mach-Zehnder interferometer. Since this fiber is considered as an optically homogenous phase object, the optical path length "Γ(x, y)" is a product of the object refractive index and its transverse dimension (*i.e.*, along the optical axis). Therefore, the optical path length difference "δ(x, y)" in the given fiber between the beam transmitted in it and that transmitted in its surrounding medium of index refraction $\mathbf{n_L}$ can be expressed by [14]:

$$\delta(\mathrm{x},\mathrm{y}) = \frac{\eta(\mathrm{x})}{\boldsymbol{\kappa}}\boldsymbol{\lambda} = 2(\mathbf{n}_{\mathrm{cl}} - \mathbf{n}_{\mathrm{L}})\xi_{\mathrm{cl}}(\mathrm{x}) + (\mathbf{n}_{\mathrm{c}} - \mathbf{n}_{\mathrm{cl}})\zeta_{\mathrm{c}}(\mathrm{x}) \tag{3}$$

Where λ is the wavelength of monochromatic light used, η(x) is the fringe shift inside the fiber at distance x from the center of fiber, κ is the liquid interfringe spacing, and ξ_{cl}(x) and ζ_c(x) are given as follows:

and

$$\left.\begin{aligned} \xi_{\mathrm{cl}}(\mathrm{x}) &= (\mathbf{r}_{\mathrm{f}}^2 - \mathbf{x}^2)^{1/2}, \\ \zeta_{\mathrm{c}}(\mathrm{x}) &= \pm\rho_1\left[1 - \left(\frac{\mathbf{x}}{\rho_2}\right)^2\right]^{1/2} \end{aligned}\right\} \tag{4}$$

The first term is applicable only in the range $-r_f \leqslant x \geqslant r_f$ and the second term is applicable only in the range $-\rho_1 \leqslant x \geqslant \rho_2$.

(ii) In this case, we assume that the major axis of elliptical core makes an angle θ with the Y-axis as shown in Figure 3b. When this fiber is placed into one of the branches of the Mach-Zehnder interferometer, the optical path length difference "δ(x, y)" is given

by the same Eq. (3) but the fiber core transversal dimension $\zeta_c(\mathrm{x})$ can be derived as follows:
as shown in Figure 3b it is observed that

$$\left.\begin{array}{ll}\mathbf{x}_1 = \mathbf{x}\cos(\theta) - \mathbf{y}\sin(\theta) & \text{a)}\\ \mathbf{y}_1 = \mathbf{y}\cos(\theta) + \mathbf{x}\sin(\theta) & \text{b)}\\ \mathbf{y}_1 = \pm\rho_1\left(1-\frac{\mathrm{x}_1^2}{\rho_2^2}\right)^{1/2} & \text{c)}\end{array}\right\} \tag{5}$$

or

$$\left.\begin{array}{ll}\mathbf{x} = \mathbf{x}_1\cos(\theta) + \mathbf{y}_1\sin(\theta) & \text{a)}\\ \mathbf{y} = \mathbf{y}_1\cos(\theta) - \mathbf{x}_1\sin(\theta) & \text{b)}\end{array}\right\} \tag{6}$$

Using Eqs. (5a) and (5c) and substituting in Eq. (6b), we get

$$\left.\begin{array}{l}(\mathbf{y}^2-\mathbf{x}^2)\cos^2(\theta) + 2\mathbf{xy}\sin(\theta)\cos(\theta) + \mathbf{x}^2 = \frac{\rho_1^2(\mathbf{y}^2-\mathbf{x}^2)\cos^2(\theta)}{\rho_2^2}\\ \qquad + \frac{2\rho_1^2\mathbf{xy}\sin(\theta)\cos(\theta)+(\rho_2^2-\mathbf{y}^2)\rho_1^2}{\rho_2^2}\end{array}\right\} \tag{7}$$

The solutions of Eq. (7) are given as follow:

$$\left.\begin{array}{l}\mathbf{y}_1(\mathbf{x}) = \frac{|\rho_1\rho_2|\mathrm{SQRT}\left[(\rho_2^2-\rho_1^2)\cos^2(\theta)-\mathbf{x}^2+\rho_1^2\right]+\mathbf{x}(\rho_1^2-\rho_2^2)\cos(\theta)\sin(\theta)}{\rho_1^2-(\rho_1^2-\rho_2^2)\cos^2(\theta)},\\ \text{and}\\ \mathbf{y}_2(\mathbf{x}) = \frac{|\rho_1\rho_2|\mathrm{SQRT}\left[(\rho_2^2-\rho_1^2)\cos^2(\theta)-\mathbf{x}^2+\rho_1^2\right]+\mathbf{x}(\rho_2^2-\rho_1^2)\cos(\theta)\sin(\theta)}{(\rho_1^2-\rho_2^2)\cos^2(\theta)-\rho_1^2}\end{array}\right\} \tag{8}$$

Then the value of $\zeta_c(\mathrm{x})$ of Eq. (3) can be calculated as follows

$$\zeta_c(\mathrm{x}) = \mathbf{y}_1(\mathrm{x}) - \mathbf{y}_2(\mathrm{x}) \tag{9}$$

The first term in Eq. (3) is still considered only in the range $-r_f \leqslant x \geqslant r_f$ but the second term will be considered only in the range $-\sigma_2 \leqslant x \geqslant \sigma_2$. The value of σ_2 can be determined as follows: By solving Eq. (7), we can get;

$$\mathbf{x} = \frac{|\rho_1\rho_2|\mathrm{SQRT}[(\rho_2^2-\rho_1^2)\mathbf{cos}^2(\theta)-\mathbf{y}^2+\rho_2^2]\pm\mathbf{y}(\rho_1^2-\rho_2^2)\mathbf{cos}(\theta)\mathbf{sin}(\theta)}{(\rho_1^2-\rho_2^2)\mathbf{cos}^2(\theta)+\rho_2^2} \tag{10}$$

By differentiating Eq. (10), where the variable is y and the value of x at point (σ_2, y) is constant, we can get,

$$\mathbf{y} = \pm\mathrm{SQRT}\left[\frac{[(\rho_1^2-\rho_2^2)\mathbf{cos}^2(\theta)+\rho_2^2]}{(\rho_1^2-\rho_2^2)^2\mathbf{sin}^2(\theta)\mathbf{cos}^2(\theta)+\rho_1^2\rho_2^2}\right]|(\rho_1^2-\rho_2^2)\mathbf{sin}(\theta)\mathbf{cos}(\theta)| \tag{11}$$

Substituting for value of y (Eq. (11)) into Eq. (10), the value of the minor axis σ_2 of the elliptical core can be given as follows:

$$\left.\begin{aligned} &\sigma_2 = \mathrm{SQRT}\left(\frac{(\rho_1^2-\rho_2^2)^2\cos^2(\theta)\sin^2(\theta)+\rho_1^2\rho_2^2}{(\rho_1^2-\rho_2^2)\cos^2(\theta)+\rho_2^2}\right) \\ \text{or} \quad &\sigma_2 = \rho_2\left[\cos^2\theta+\frac{\rho_1^2}{\rho_2^2}\sin^2\theta\right]^{1/2} \end{aligned}\right\} \tag{12}$$

(iii) In this case, we assume that the major axis ρ_1 of elliptical core makes an angle θ with the Y-axis and the elliptical core center is shifted away from the fiber center by C and (C_1, C_2) from fiber glass axes (X, Y) as shown in Figure 3c. Where, $\mathbf{C_1} = \mathbf{C}\ \mathbf{sin}(\theta)$ and $\mathbf{C_2} = \mathbf{C}\ \mathbf{cos}(\theta)$. The optical path length difference "δ(x, y)" is given by the same Eq. (3) but the fiber core transversal dimension ζ_c(x) is given by

$$\zeta_c(\mathrm{x}) = \mathbf{y}'(\mathrm{x})_1 - \mathbf{y}'_2(\mathrm{x}) \tag{13}$$

Where,

$$\left.\begin{aligned} &\mathbf{y}'_1(\mathrm{x}) = \frac{|\rho_1\rho_2|\mathrm{SQRT}\left[(\rho_2^2-\rho_1^2)\cos^2(\theta)-(\mathrm{x}-\mathrm{C}_1)^2+\rho_1^2\right]+(\mathrm{x}-\mathrm{C}_1)(\rho_1^2-\rho_2^2)\cos(\theta)\sin(\theta)}{\rho_1^2-(\rho_1^2-\rho_2^2)\cos^2(\theta)}+\mathrm{C}_2, \\ \text{and} \\ &\mathbf{y}'_2(\mathrm{x}) = \frac{|\rho_1\rho_2|\mathrm{SQRT}\left[(\rho_2^2-\rho_1^2)\cos^2(\theta)-(\mathrm{x}-\mathrm{C}_1)^2+\rho_1^2\right]+(\mathrm{x}-\mathrm{C}_1)(\rho_2^2-\rho_1^2)\cos(\theta)\sin(\theta)}{(\rho_1^2-\rho_2^2)\cos^2(\theta)-\rho_1^2}+\mathrm{C}_2 \end{aligned}\right\} \tag{14}$$

For this case, the first term in Eq. (3) is applicable in the range $-r_f \leqslant x \geqslant r_f$ and the second term is applicable in the range $A \leqslant x \geqslant B$. Where A and B are constant and can be written as follows:

$$\left.\begin{aligned} &\mathbf{A} = \mathbf{C}_1 - \sigma_2, \\ \text{and} \quad &\mathbf{B} = \mathbf{C}_1 + \sigma_2 \end{aligned}\right\} \tag{15}$$

Now we will generalize this interference formula when a cylindrical fiber of $\mathbf{r_f}$ having an identical multi-elliptical core ($\mathbf{N}$ cores; in our case $\mathbf{N} = \mathbf{9}$) distributed around of the circle of radius $\mathbf{C}$ from the fiber center, as shown in Figure 2, is introduced in one of the optical paths of the Mach-Zehnder interferometer. The relation between optical path length difference "δ(x, y)" in the given fiber and the refractive index distribution along the fiber radius can be written as follows:

$$\delta(\mathrm{x},\mathrm{y}) = \frac{\eta(\mathrm{x})}{\boldsymbol{\kappa}}\boldsymbol{\lambda} = 2(\mathbf{n}_{\mathrm{cl}} - \mathbf{n}_{\mathrm{L}})\xi_{\mathrm{cl}}(\mathrm{x}) + (\mathbf{n}_{\mathrm{c}} - \mathbf{n}_{\mathrm{cl}})\zeta^*_{\mathrm{c}}(\mathrm{x}) \tag{16}$$

where

$$\zeta^*_{\mathrm{c}}(\mathrm{x}) = \mathbf{y}''_1(\mathrm{x}) - \mathbf{y}''_2(\mathrm{x}) \tag{17}$$

where,

$$\left.\begin{aligned}
\mathbf{y}''_1(\mathrm{x}) &= \sum_{\mathrm{i}=1}^{\mathrm{N}} \frac{|\rho_1\rho_2|\mathrm{SQRT}\left[(\rho_2^2-\rho_1^2)\cos^2(\theta_\mathrm{i})-(\mathrm{x}-\mathrm{C}_{1\mathrm{i}})^2+\rho_1^2\right]+(\mathrm{x}-\mathrm{C}_{1\mathrm{i}})(\rho_1^2-\rho_2^2)\cos(\theta_\mathrm{i})\sin(\theta_\mathrm{i})}{\rho_1^2-(\rho_1^2-\rho_2^2)\cos^2(\theta_\mathrm{i})} + \mathrm{C}_{2\mathrm{i}}, \\
&\text{and} \\
\mathbf{y}''_2(\mathrm{x}) &= \sum_{\mathrm{i}=1}^{\mathrm{N}} \frac{|\rho_1\rho_2|\mathrm{SQRT}\left[(\rho_2^2-\rho_1^2)\cos^2(\theta_\mathrm{i})-(\mathrm{x}-\mathrm{C}_{1\mathrm{i}})^2+\rho_1^2\right]+(\mathrm{x}-\mathrm{C}_{1\mathrm{i}})(\rho_2^2-\rho_1^2)\cos(\theta_\mathrm{I})\sin(\theta_\mathrm{i})}{(\rho_1^2-\rho_2^2)\cos^2(\theta_\mathrm{i})-\rho_1^2} + \mathrm{C}_{2\mathrm{i}}
\end{aligned}\right\} \tag{18}$$

where, $\mathbf{C_{1i}} = \mathbf{C}\ \mathbf{sin}(\theta_\mathbf{i})$, and $\mathbf{C_{2i}} = \mathbf{C}\ \mathbf{cos}(\theta_\mathbf{i})$.

In the present work, the number of identical elliptical cores are **nine** and the angle between each two neighbour cores is **40** deg., *i.e.,* $\theta_\mathbf{i} = \mathbf{0}$, **40**, **80**, **120**, and **160** as shown in Figure 2.

The second term of Eq. (16) is applicable in the range $A_i \leqslant x \geqslant B_i$. Where A_i and B_i are constant and can be written as follows:

$$\left.\begin{aligned}
\mathbf{A}_\mathrm{i} &= \mathbf{C}_{1\mathrm{i}} - \sigma_{2\mathrm{i}}, \\
&\text{and} \\
\mathbf{B}_\mathrm{i} &= \mathbf{C}_{1\mathrm{i}} + \sigma_{2\mathrm{i}}
\end{aligned}\right\} \tag{19}$$

Where,

$$\left.\begin{aligned}
\sigma_{2\mathrm{i}} &= \mathrm{SQRT}\left(\frac{(\rho_1^2-\rho_2^2)^2\cos^2(\theta_\mathrm{i})\sin^2(\theta_\mathrm{i})+\rho_1^2\rho_2^2}{(\rho_1^2-\rho_2^2)\cos^2(\theta_\mathrm{i})+\rho_2^2}\right) \\
&\text{or} \\
\sigma_{2\mathrm{i}} &= \rho_2\left[\cos^2\theta_\mathrm{i} + \frac{\rho_1^2}{\rho_2^2}\sin^2\theta_\mathrm{i}\right]^{1/2}
\end{aligned}\right\} \tag{20}$$

The interference formula (Eq. (16)) describes the interference pattern that is observed in the exit plane of the transverse Mach-Zehnder interferometer, where the identical nine-elliptical core fiber under study is investigated.

In general, the optical fiber users require and the fabrication process assures that the fiber parameters are stable along its length. In such circumstances, the fiber parameters are constant over its length within the field of view of the interferometer. For this reason, the aim of the present work is that computer-aide Mach-Zehnder interferometer applied to extract the phase shift data from different interferogram points along the fiber radius (axis) and Eq. (16) be used to finally characterize the fiber in any intermediate point. Having determined the refractive indices, maximum index difference and geometrical dimensions, the precise detection of possible structural microdefects of multi-elliptical core optical fibers can be done *via* their fringe shift distribution along their lengths.

EXPERIMENTAL RESULTS AND DISCUSSION

The maximum refractive index difference, the index profile, and fiber geometry are important in characterizing both multimode and monomode fiber transmission behavior. In the present work, the above optical and geometrical parameters will be determine for identical nine-elliptical core glass fiber. The fiber cladding of radius $\mathbf{r}_f = 190$ μm and core radii $\rho_1 = 16$ μm (major) and $\rho_2 = 8$ μm (minor). The geometrical parameters of the nine-elliptical optical fiber are determined using transverse microscope as shown in Table 1. The interferometer is aligned to produce straight parallel background fringes (liquid fringes, the fiber is absence) as shown in Figure 1. Figure 4a displays a photograph of an identical nine-elliptical core fiber cross-section; photo enlarg. 144x. This fiber is placed in liquid quartz cell ($\mathbf{n}_L$) inside one of the optical paths of Mach-Zehnder interferometer. The fiber will be illuminated transversally to its axis. Therefore, the background fringes will be perturbed by the presence of this fiber (for example, see Fig. 4b, $\mathbf{n}_L = 1.591$). A certain rotating disk **RD** that has a specific

TABLE 1 The Geometrical Parameters of the Nine-Elliptical Optical Fiber

i	θ_i	σ_{2i} (μm)	C_{1i} (μm)	C_{2i} (μm)	A_i (μm)	B_i (μm)
1	0	$\rho_2 = 8$	0	45	− 8	8
2	40	11.972	28.925	34.472	16.953	40.897
3	80	15.818	44.316	7.814	28.498	60.134
4	120	14.422	38.971	− 22.500	24.549	53.393
5	160	9.298	15.931	− 42.286	6.092	24.689

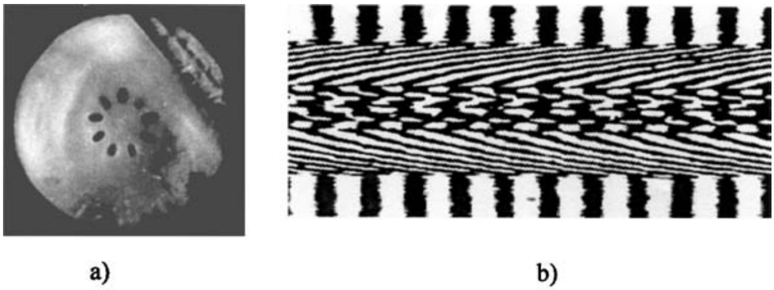

FIGURE 4 a) Photography of a nine-elliptical core optical fiber cross-section; photo enlarg. 144x; b) Interferogram of nine-elliptical core fiber, exposed for the investigation; $n_L = 1.591$ and $\lambda = 632.8$ nm.

mechanism is used to measure the fringe shift $\eta(x)$ in a selected elliptical core. Particularly the elliptical core of a major axis ρ_1 that makes an angle ($\theta = \mathbf{0}°$) with respect to the optical axis of the system (Y-axis, see Fig. 2). Fulfilling the selecting region can be done by turning the fiber round its main axis through an angle arising from its geometry (Fig. 2).

In order to increase the accuracy of the measurements it is necessary to couple the Mach-Zehnder interferometer to an image proces-

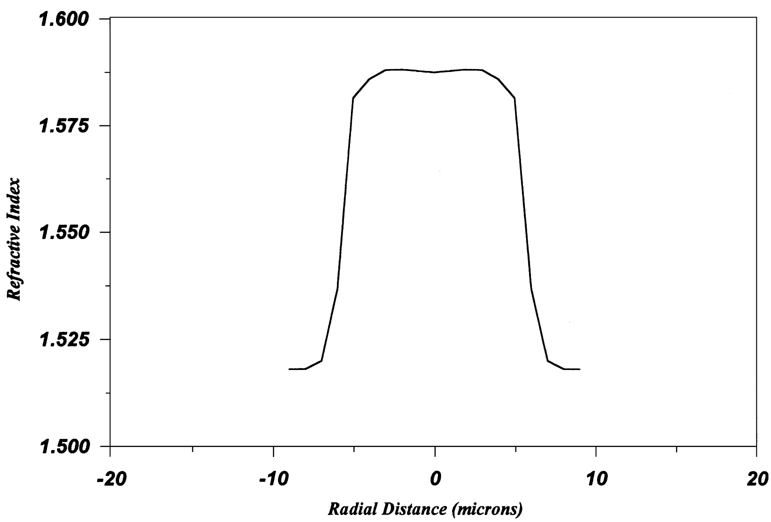

FIGURE 5 Displays the refractive index profile of the core, which is made an angle $\theta = 0.0$ deg. with Y-axis, of nine-elliptical core fiber, $n_L = n_{cl} = 1.518$ and $\lambda = 632.8$ nm.

sing system *via* a CCD camera (see Fig. 1). The captured interferograms can be filtered if necessary. All experimental data are extracted and processed by **PC** compatible computer equipped with a framegrabber. The measurements are performed between as many fringes as possible and the result averaged to improve the precision. The liquid interfringe spacing κ and the fiber fringe shift $\eta(x)$ can be determined by employing the intensity scanning along line vector (intensity distribution measurement) perpendicular to the liquid fringe. By selecting a matching liquid to have refractive index $\mathbf{n_L}$ equal to the cladding refractive $\mathbf{n_{cl}}$ ($n_{cl} = n_L = 1.518$) the refractive index profile can be determined for the fiber core (see Fig. 5, $n_c = 1.578$). Having determined the refractive indices n_{cl} & n_c and geometrical parameters of the optical fiber and applying of interference formula (Eq. (16)), the expected fringe shift distribution along its radius for any immersion liquid can be determined. Finally, it is important to note that this method not only gives information on refractive indices of the fibers but also visualizes any irregularity in the fiber structure in terms of the distortion of the fringes.

CONCLUSIONS

In the present work, a general interference formula that can describe the interference pattern of multi-core optical fiber in a transverse interferometer is presented. This formula represents the optical path difference through multi-elliptical core optical fibers (with respect to the radial position in the observation plane). Therefore, this formula with Mach-Zehnder interferometry has been used to characterize an identical nine-elliptical core optical fiber *via* its refractive index measurement. The fringe field interference pattern that are observed in the image plane of the Mach-Zehnder interferometer has been processed automatically to measure the fringe shift within the fiber. The advantage of the present method is that the evaluation is simple and the results are satisfactory precise. Additionally, this method is suitable for quick and precise detection of irregularities of the geometrical shape of the multi-core optical fiber under study *via* their fringe shift distribution along their length.

REFERENCES

[1] Presby, H. M., Mammel, H. M. and Derosier, R. M. (1976). *Rev. Sci. Instr.*, **47**, 384.
[2] Stone, J. and Earl, H. E. (1978). *Appl. Opt.*, **17**, 3647.
[3] Marhic, M. E., Ho, P. S. and Epstein, N. (1975). *Appl. Phys. Lett.*, **26**(10), 574.
[4] Presby, H. M., Marcuse, D. and Cohen, L. G. (1979). Part 2, *Appl. Opt.*, **18**, 3249.

[5] Kokubun, Y. and Iga, K. (1977). *Trans. IECE Japan*, **E60**, 3249.
[6] Yong, M. (1981). *Appl. Opt.*, **20**(19), 3415.
[7] Iga, K. and Kokubun, Y. (1978). *Appl. Opt.*, **17**, 1972.
[8] Sochacki, J. (1986). *Appl. Opt.*, **25**, 3473.
[9] Pluta, M. (1979). *Optical Fibers and Their Application II*, Polish Academy of Science, 148, Warsaw.
[10] Stewart, W. J. (1977). *Tech. Dig. 100c* (IECE Tokyo) p. 395.
[11] Bozyk, M. (1989). *SPIE*, **1121**, 284.
[12] Simpson, J. R. (1976). *Appl. Opt.*, **15**, 1048.
[13] Sochacka, M. (1992). "Phase stepping approach to data acquisition for refractive index profiling of GRIN optical fibers", *Proceedings of the X Topical Meeting on Gradient Index Optical Elements and Systems*, Santiago de Compostela, Spain.
[14] Sokkar, T. Z. N. (1992). *Appl. Opt.*, **31**(9), 1229.
[15] Barakat, N., Hamza, A. A. and Gonid A. S. (1985). *Appl. Opt.*, **24**, p. 4383.
[16] Barakat, N. and Hamza, A. A. (1990). "*Interferometry of Fibrous Material*", Adam Hilger, Bristol.